Inorganic Chemistry

Article

pubs.acs.org/IC

Insertion of a Transient Tin Nitride into Carbon−Carbon and Boron−Carbon Bonds

Shuai Wang,[†] Lizhi Tao,[†] Troy A. Stich,[†] Marilyn M. Olmstead,[†] R. David Britt,[†] and Philip P. Power*

[†]Department of Chemistry, University of California Davis, 1 Shields Avenue, Davis, California 95616, United States

Supporting Information

ABSTRACT: A simple exchange reaction between $[Ar^{iPr4}Sn(\mu\text{-}Cl)]_2$ (**1**) and sodium azide afforded the doubly bridged Sn(II) azide, $[Ar^{iPr4}Sn(\mu\text{-}N_3)]_2$ (**2**) (Ar^{iPr4} = C_6H_3-2,6(C_6H_3-2,6-$^i Pr_2$)$_2$) in 85% yield. Photolysis of a diethyl ether solution of **2** for ca. 16 h yielded an azepinyl-substituted insertion product, [C_6H_3-2-(C_6H_3-2,6-$^i Pr_2$)-6-(C_6H_3N-3,7-$^i Pr_2$)Sn]$_2$ (**3**). The reaction of the Lewis acid, $B(C_6F_5)_3$ (BCF), or the Lewis base, pyridine, with **2** dissociates the dimer to afford the corresponding complexed monomeric Sn(II) azide, $Ar^{iPr4}SnN_3BCF$ (**4**) in which BCF coordinates the α-nitrogen, or $Ar^{iPr4}Sn$(pyridine)N_3 (**6**) in which pyridine coordinates to the tin atom. Photolysis of **4** in diethyl ether for 12 h results in the insertion of the α-nitrogen of the azide group into one of the B−C bonds of the BCF acceptor to yield the tin(II) amide, $Ar^{iPr4}SnN(C_6F_5)B(C_6F_5)_2$ (**5**). In contrast, photolysis of **6** for over 36 h afforded no apparent reaction. A highly reactive Sn nitride intermediate, $Ar^{iPr4}Sn{\equiv}N$, is proposed as part of the mechanistic pathway for the formation of **3** and **5** as a result of trapping the tin-centered radical isomers. This was effected by immediate freezing the samples of **2** or **4** after ca. 30 min of UV photolysis and recording their electron paramagnetic resonance spectra. These exhibited a rhombic g tensor of [g_1, g_2, g_3] = [2.029, 1.978, 1.933]. This radical intermediate could be related to the valence isomers of the nitride [$-Sn^{IV}{\equiv}N$] intermediate, in isomeric equilibrium with the nitrene [$-Sn^{II}-N$] and nitridyl [$-Sn^{III}{=}N\cdot$] forms, but with the spin density on the nitrogen being quenched, possibly by the H atom abstraction to form an S = 1/2 species of formula $-Sn\cdot{=}N(H)$.

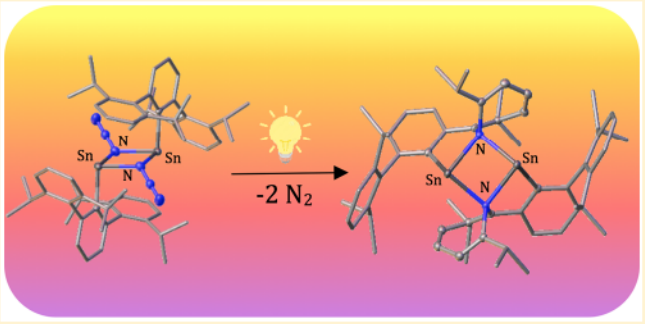

INTRODUCTION

The study of metal azide chemistry has focused mainly on derivatives of the transition metals,[1−3] and the structures and reactivity of a range of such complexes are well-established.[4,5] An interesting feature of their reactivity is decomposition to metal nitrides, such as $MoNCl_3$ or $WNCl_3$, via thermolysis of the azido metal halides MCl_5N_3 (M = Mo, W) with elimination of N_2 and Cl_2.[6] Related azido metal complexes of formula MCl_4N_3 (M = Nb, Ta) were shown to react with PPh_3 to give phosphoraneiminato complexes $Cl_4M{=}N{=}PPh_3$ with elimination of N_2.[7,8] Azido complexes have also been used as precursors for homo- or heterometallic clusters. An example is the gold cluster $[(Ph_3PAu)_8]^{2+}$, obtained via photolytic decomposition of $[R_3PAuN_3]$ in tetrahydrofuran (THF) solution at room temperature.[9] Azido ligands are also encountered as bridging ligands in transition-metal clusters, such as $[Ti_4(O^iPr)_{12}(N_3)_4]$, which were obtained by reacting $(N_3)_2Ti(O^iPr)_2$ with $Ti(O^iPr)_4$ at 135 °C.[10]

In the main-group elements, heavy group 14 metal(IV) azides have been studied in connection with their photochemical reactivity and use in organic synthesis. Reichle first reported the Curtius-type rearrangement in 1964, where a carboxylate azide thermally decomposes to produce isocyanate (Scheme 1, top).[11,12] The thermolysis of Ph_3SiN_3 results in migration of the phenyl group from Si to the α-nitrogen atom of the azide and eliminates N_2 to afford the silaimine $Ph_2Si{=}NPh$ as an intermediate, which is trapped by reaction with aldehydes or ketones in a pseudo-Wittig manner to afford an imine and cyclotrisiloxane (Scheme 1 middle).[13] Group 14 metal(IV) azides R_3EN_3 (E = Si, Ge, Sn) have also been shown to undergo cycloaddition with acetylene to give triazole via a click mechanism (Scheme 1, bottom).[14−16] In contrast, only a few structurally characterized low-valent group

Scheme 1. Some Reactivity Studies of Group 14 Azides[20−25]

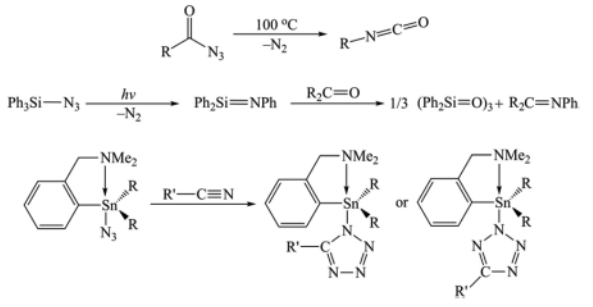

Received: September 20, 2017
Published: November 13, 2017

DOI: 10.1021/acs.inorgchem.7b02413
Inorg. Chem. 2017, 56, 14596−14604

14 azides have been reported since the first low-valent heteroleptic group 14 azide Tp′GeN_3 (Tp′ = hydrotris(3,5-dimethylpyrazol-1-yl)borato) was reported by Filippou and co-workers in 1998.[17]

Most of these azide derivatives are monomeric and are supported by the bidentate ligands ((^{n}Pr)$_2$ATI (ATI = aminotroponiminate),[18] (Mes)$_2$DAP (DAP = diazapentadienyl),[19] or [t-BuO(Me$_2$)Si]$_2$N)[20] or tridentate ligand (Tp′ or CpCo{P(O)(OEt)$_2$}$_3$).[21] Recently, Inoue and co-workers reported the synthesis and structure of the dimeric terminal Sn(II) azide, [NIPrSn(μ-N_3)]$_2$ (NIPr = bis(2,6-diisopropylphenyl)imidazolin-2-imine).[22] However, the reactivity of such species has not been investigated.

In parallel with the azido complexes, the transition-metal nitrides have been studied for more than a century.[23] They have been synthesized by several routes that include the above-mentioned decomposition of metal azide with dinitrogen elimination,[6,24] ammonolysis reactions of transition-metal oxides, such as OsO_4 or Re_2O_7 with NH_3 or ammonium salts,[25,26] reactions of transition-metal carbonyls or halides with NCl_3,[27,28] or of transition-metal oxo complexes such as $ReOCl_3(PR_3)$ with hydrazine in the presence of ethanol.[29,30] Numerous complexes featuring terminal M≡N triple bonds have been reported. Recently, a terminal actinide nitride species, [U(N)(Tren^{TIPS})] (Tren^{TIPS} = {N(CH$_2$CH$_2$NSi^{i}Pr$_3$)$_3$}$_3^-$, ^{i}Pr = CH(CH$_3$)$_2$), was synthesized from [U(Cl)(Tren^{TIPS})] via a mild redox route, involving alkali metal reduction, formation of Na-bridged U(V) nitride, and iodine oxidation.[31]

Stable main-group metal nitrides with triple bonds to nitrogen are scarce, and none is known for the group 14 elements. However, in the group 15 and 16 elements, heteroatomic triple bonds between nitrogen and these elements are known; these include iminophosphenium ions, [Mes*N≡P]$^+$ (Mes* = C$_6$H$_2$-2,4,6-^{t}Bu$_3$),[31,32] substituted thiazyne, PhRR′S≡N,[33] and the thionitrosyl-coordinated transition-metal complexes, such as [Tc(NS)(S$_2$CNEt$_2$)$_2$Br$_2$],[34] TpOs(NS)Cl$_2$ (Tp = hydrotris(1-pyrazolyl)borate),[35] and [Ni(NSF$_2$NMe$_2$)$_6$](AsF$_6$)$_2$,[36] which have been structurally and spectroscopically investigated. Recently, Inuoe and co-workers attempted to use B(C$_6$F$_5$)$_3$ to extrude a carbene moiety from Sn{N═CN(Dipp)CHCHN-(Dipp)}{N(SiMe$_3$)$_2$} (Dipp = C$_6$H$_3$-2,6-^{i}Pr$_2$) to generate a Sn≡N triple-bonded species. This product led to further reaction and extraction of the methyl group of the −N(SiMe$_3$)$_2$ ligand to give an amino(imino) silylene bridged Sn(II) cation, [:SnN = CN(Dipp)CHCHN(Dipp)(NSiMe$_3$)(μ-SiMe$_2$)][MeB(C$_6$F$_5$)$_3$].[22] Recently, Kato and co-workers attempted to synthesize a silanitrile via a reaction of a phosphine-stabilized chlorosilylene with NaN_3 followed by decomposition. Instead, a 1,3-disila-2,4-diazacyclobutadiene was obtained, which was deemed to be formed by dimerization of the monomeric silanitrile.[37]

We now report the investigation of the structure and reactivity of the low-valent bridged aryl tin(II) azide [Ar^{iPr4}Sn(μ-N_3)]$_2$ (2) (Ar^{iPr4} = C$_6$H$_3$-2,6(C$_6$H$_3$-2,6-^{i}Pr$_2$)$_2$). This species is shown to eliminate N_2 under UV irradiation with insertion of the α-nitrogen into a C−C bond from a flanking phenyl ring of the terphenyl ligand to afford a peculiar aryl/azepinyl tin(II) product [C$_6$H$_3$-2-(C$_6$H$_3$-2,6-^{i}Pr$_2$)-6-(C$_6$H$_3$N-3,7-^{i}Pr$_2$)Sn]$_2$ (3) (Scheme 2).

The photochemical reactivity of the azide was further investigated via the reaction of a Lewis acid, that is, B(C$_6$F$_5$)$_3$ (BCF), and a Lewis base, pyridine, to complex the azido species. This generated the two monomeric complexes Ar^{iPr4}SnN$_3$BCF (4) and Ar^{iPr4}Sn(pyridine)N$_3$ (6). Photolysis of 4 eliminates N_2, and the B−C(phenyl) bond is cleaved via nitrogen insertion

Scheme 2. Synthesis of the Low-Valent Azido Sn(II) Compound 2, Its Photolysis to Give 3, Its Reaction with the Lewis Acid, Tris(pentafluorophenyl)borane (BCF), to yield 4,[a] or with the Lewis Base, Pyridine to Yield 6

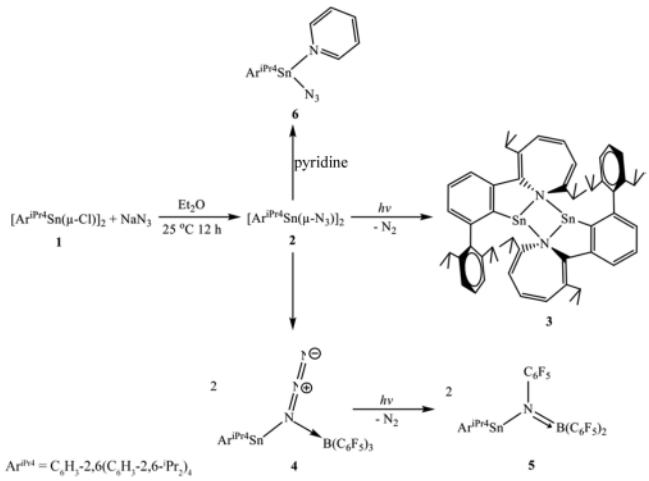

[a]Further photolysis of 4 yielded the B−C inserted species 5.

to afford the amido derivative, Ar^{iPr4}SnN(C$_6$F$_5$)B(C$_6$F$_5$)$_2$ (5). The putative tin nitride was characterized by electron paramagnetic resonance (EPR) spectroscopy.

RESULTS AND DISCUSSION

Synthesis. Mixing [Ar^{iPr4}Sn(μ-Cl)]$_2$ and 1.5 equiv of NaN_3 in diethyl ether at room temperature afforded a dark yellow solution, from which the product [Ar^{iPr4}Sn(μ-N_3)]$_2$ (2) was obtained at ca. −18 °C as colorless crystals in 85% yield. UV irradiation of a diethyl ether solution of 2 for 12 h yielded an orange solution, from which 3 was crystallized at ca. −18 °C, also as a colorless solid in 84% yield. The X-ray crystal structure of 3 shows that dinitrogen has been eliminated and the remaining tin-bound α-nitrogen atom has been inserted into one of the flanking -C$_6$H$_3$-2,6-^{i}Pr$_2$ rings of the terphenyl ligand to give an aryl/azepinyl tin(II) species [C$_6$H$_3$-2-(C$_6$H$_3$-2,6-^{i}Pr$_2$)-6-(C$_6$H$_3$N-3,7-^{i}Pr$_2$)Sn]$_2$ (3). An attempt to stabilize the potential Sn−N multiple-bonded nitride intermediate by the addition of a Lewis acid B(C$_6$F$_5$)$_3$ (BCF) to 2 afforded the complex Ar^{iPr4}SnN$_3$(BCF) (4), in which the boron is coordinated by the α-nitrogen atom of the azido group. A dark orange solution was obtained after exposing 4 under UV light for 12 h. In this case, one of the B−C bonds was cleaved by α-nitrogen atom insertion to form the amide Ar^{iPr4}SnN(C$_6$F$_5$)B(C$_6$F$_5$)$_2$ (5) in 92% yield. Reaction of 2 with a Lewis base, pyridine (py), led to a colorless product Ar^{iPr4}Sn(py)N$_3$ (6) in which a pyridine is coordinated to the tin atom. Exposure of 6 under UV light for 12 h afforded no reaction, suggesting that the pyridine that binds via the empty orbital on the Sn atom blocks further reaction at tin.

Structures. The symmetric aryl/azido distannene dimer [Ar^{iPr4}Sn(μ-N_3)]$_2$ (2) (Figure 1) was obtained as coloress crystals from Et$_2$O solution at ca. −18 °C. The structure is characterized by a center of symmetry in the center of the Sn_2N_2 ring. The tin atoms have pyramidal coordination (Σ°Sn = 270.2°), with the Sn−C(ipso) distance of 2.254(12) Å. The azido group bridges the tin atoms via the α-nitrogen atom (i.e., N(1)) with the Sn(1)−N(1) and Sn(1)−N(1a) distances of 2.268(13) and 2.360(12) Å, which are significantly longer than the Sn−N bond length range of 2.110(9)−2.156(3) Å in the

DOI: 10.1021/acs.inorgchem.7b02413
Inorg. Chem. 2017, 56, 14596−14604

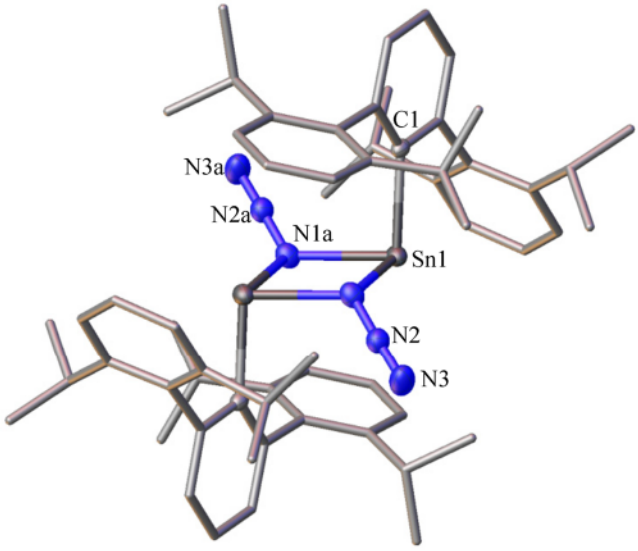

2

Figure 1. Illustration of the structure of $[Ar^{iPr4}Sn(\mu\text{-}N_3)]_2$ (2). Thermal ellipsoids (50%) are shown for the core atoms only. Hydrogen atoms are not shown. Selected bond lengths [Å] and bond angles [deg]: C(1)–Sn(1) 2.253 (13), Sn(1)–N(1) 2.268 (13), Sn(1)–N(1a) 2.360 (11), N(1)–N(2) 1.244 (7), N(2)–N(3) 1.138 (7), C(1)–Sn(1)–N(1) 92.7 (4), C(1)–Sn(1)–N(1a) 104.8 (3), N(1)–Sn(1)–N(1a) 72.8 (3), Sn(1)–N(1)–Sn(1a) 107.2 (3), N(1)–N(2)–N(3) 178.6 (9), N(2)–N(1)–Sn(1) 118.9 (16), N(2)–N(1)–Sn(1a) 120.5 (15).

terminal tin(II) azide species such as $[(Pr^n)_2ATI]SnN_3$ (ATI = aminotroponiminate), $[HB(3,5\text{-}(CF_3)_2Pz)_3]AgSn(N_3)$-$[(^nPr)_2ATI]$ (Pz = pyrazole), and $[(Mes)_2DAP]SnN_3$ (DAP = diazapentadienyl).[18,19,21] The azide moiety shows an almost linear geometry with a N(1)–N(2)–N(3) bond angle of 178.6(9)°. The N(1)–N(2) moiety subtends an angle of 146.5 (8)° with respect to the Sn_2N_2 plane, which is within the range of those in other doubly bridged main-group metal azido species $[(\eta^1\text{-}Cp^*)Ga(\mu_2\text{-}N_3)\{N(SiMe_3)_2\}]_2$ (131.5 (7)°, Cp* = pentamethylcyclopentadienyl) and $[^tBuOMe_2Si]_2NGeN_3$ (159.2 (3)°).[20,38]

The symmetric aryl/azepinyl distannene $[C_6H_3\text{-}2\text{-}(C_6H_3\text{-}2,6\text{-}^iPr_2)\text{-}6\text{-}(C_6H_3N\text{-}3,7\text{-}^iPr_2)Sn]_2$ (3) was isolated as colorless crystals from a diethyl ether solution at ca. −18 °C. The structure (Figure 2) has a center of symmetry at the center of the Sn_2N_2 ring. Each tin atom has a distorted trigonal pyramidal coordination with a narrow C(1)–Sn(1)–N(1) angle of 77.3 (11)°. The nitrogen atom possesses tetrahedral coordination and is bound to two tin atoms and two carbons derived from a C_α–C_β bond of one of the flanking C_6H_3 rings that forms the azepinyl group, in which the C(2)–C(3), C(4)–C(5), and C(6)–C(7) bond lengths, 1.357(5), 1.362(5), and 1.362(5) Å, lie well-within the typical C=C double bond range.[39] The N(1)–C(2) and N(1)–C(7) distances of 1.466 (4) and 1.457 (3) Å are consistent with C–N single bonding.[40]

In the crystal structure of the monomeric azido stannylene $Ar^{iPr4}SnN_3B(C_6F_5)_3$ (4) (Figure 3), the tin atom has bent coordination with a relatively narrow C(1)–Sn(1)–N(1) angle of 97.3 (2)°. Unlike the previously reported BCF coordinated transition-metal azido complexes,[41,42] in which the B atom is attached to the nitrogen atom furthest from the metal (γ-N), the boron atom is coordinated to the N(1) atom that is also bonded to B(1) and Sn(1). The Sn–N(1) distance of 2.259 (11) Å is slightly shorter than that in the doubly bridged 2; however, it is significantly longer than those in the aforementioned terminal Sn

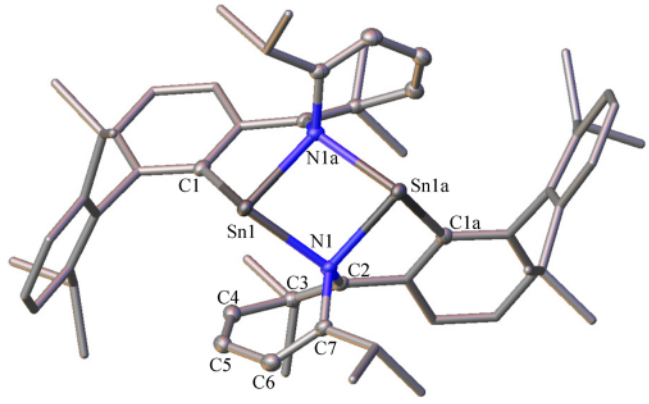

3

Figure 2. Illustration of the structure of $[C_6H_3\text{-}2\text{-}(C_6H_3\text{-}2,6\text{-}Pr^i_2)\text{-}6\text{-}(C_6H_3N\text{-}3,7\text{-}Pr^i_2)Sn]_2$ (3) Thermal ellipsoids (50%) are shown for the core atoms only. Hydrogen atoms are not shown. Selected bond lengths [Å] and bond angles [deg]: C(1)–Sn(1) 2.219 (3), Sn(1)–N(1) 2.299 (3), Sn(1)–N(1a) 2.300 (3), N(1)–C(2) 1.466 (4), N(1)–C(7) 1.457 (4), C(2)–C(3) 1.357 (5), C(3)–C(4) 1.469 (5), C(4)–C(5) 1.362 (5), C(5)–C(6) 1.451 (5), C(6)–C(7) 1.362 (5), C(1)–Sn(1)–N(1) 108.8 (11), C(1)–Sn(1)–N(1a) 77.3 (11), N(1)–Sn(1)–N(1a) 76.8 (10), Sn(1)–N(1)–Sn(2) 93.5 (10), Sn(1)–N(1)–C(7) 106.4 (19), Sn(1)–N(1)–C(2) 120.9 (2), C(2)–N(1)–C(7) 106.8 (3).

azido species (2.157 (4)–2.253 (4)).[18,19,21] The boron atom, which possesses distorted tetrahedral coordination, is bound to three C_6F_5 groups as well as the N(1) atom from the azido group with interligand angles within the range of 101.7 (18)–116.9 (3)°. The N(1)–B(1) bond distance of 1.638 (9) Å is consistent with a dative N→B interaction.[42,43]

The monomeric amido stannylene $Ar^{iPr4}SnN(C_6F_5)B(C_6F_5)_2$ (5) is the photolysis product of 4. The two-coordinate tin atom retains a bent coordination geometry but with a much wider C(1)–Sn(1)–N(1) angle of 115.2 (13)°, cf. 97.3 (2)° in 4. The coordination of the ipso-carbon atom C(1) displays a very large distortion from planarity with an angle of *ca.* 32.4° between Sn(1) and C(1) and the averaged plane of the C(1) aryl ring. This distortion is reminiscent of that in the Ge(II) bisgermylene imido species, 1-AdN$(GeAr^{iPr4})_2$ (1-Ad = 1-adamantanyl), which possesses a Ge–C angle of 35.7° with respect to the Ge_2N plane.[44] The distorted geometry at the ipso C atom is probably due to increased steric hindrance as a result of the intramolecular electronic interaction involving the F atoms of the $-C_6F_5$ moieties and the π orbital ring of the flanking phenyl group, as indicated by the close distances of 2.982 (3)–3.095 (4) Å between the phenyl rings and the F atoms. The N(1) atom, which possesses a trigonal planar geometry ($\Sigma°N$ = 359.6°), is inserted into a B–C bond from the $B(C_6F_5)_3$ group. The N(1)–B(1) distance of 1.398 (6) Å is much shorter than that in 4, as well as being shorter than a normal N–B single bond, indicating the lone pair on the N atom is delocalized onto the B atom to form a bond with multiple character. The coordination of the B(1) atom changes from four to three ($\Sigma°B = 360°$), being bound to the nitrogen atom and two carbon atoms from two C_6F_5 moieties, as a consequence of the N(1) insertion. The C(3)B(1)C(4) array is almost coplanar with the Sn(1)-N(1)C(2) plane with only a small torsion angle of 5.2 (6)°.

The crystal structure of 6 (Figure 4) displays a trigonal pyramidal geometry at the Sn atom that carries a terphenyl group, a pyridine, and an azido group with $\Sigma°Sn$ = 276.7°. Unlike 3, in which has the BCF group binds to the N(1) atom, the Lewis base, pyridine, binds to the Sn atom with a relatively

DOI: 10.1021/acs.inorgchem.7b02413
Inorg. Chem. 2017, 56, 14596–14604

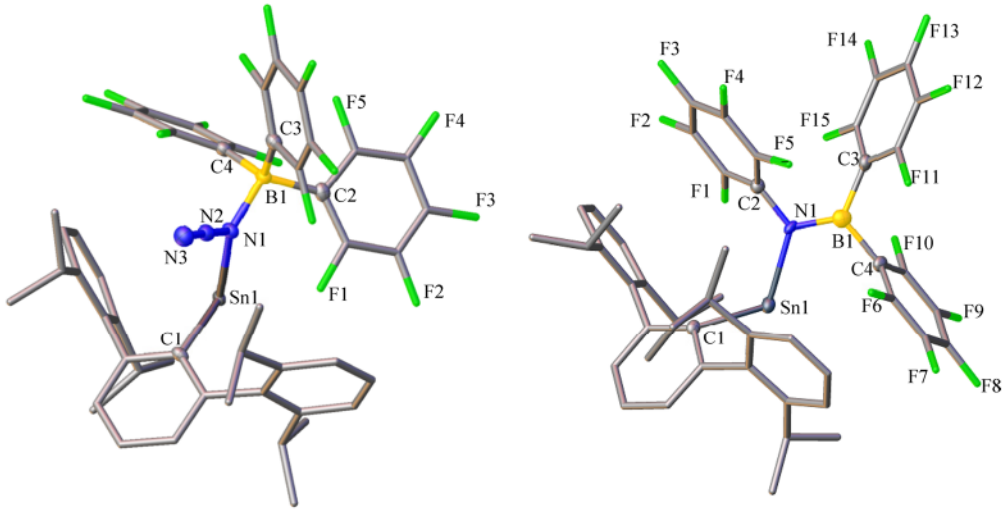

4 5

Figure 3. Illustrations of the structures of $Ar^{iPr4}SnN_3B(C_6F_5)_3$ (4) and $Ar^{iPr4}SnN(C_6F_5)B(C_6F_5)_2$ (5). Thermal ellipsoids (50%) are shown for the core atoms only. Hydrogen atoms are not shown. Selected bond lengths [Å] and bond angles [deg]: 4, Sn(1)−C(1) 2.202 (11), Sn(1)−N(1) 2.259 (11), N(1)−N(2) 1.244 (5), N(2)−N(3) 1.127 (4), N(1)−B(1) 1.638 (9), C(1)−Sn(1)−N(1) 97.3 (2), Sn(1)−N(1)−N(2) 119.2 (4), N(1)−N(2)−N(3) 177.6 (4), Sn(1)−N(1)−B(1) 120.9 (13), N(2)−N(1)−B(1) 119.4 (3), N(1)−B(1)−C(2) 109.8 (4), N(1)−B(1)−C(3) 108.1 (19), N(1)−B(1)−C(4) 101.7 (18), C(2)−B(1)−C(3) 106.1 (4), C(2)−B(1)−C(4) 114.0 (8), C(3)−B(1)−C(4) 116.9 (3); 5, Sn(1)−C(1) 2.208 (3), Sn(1)−N(1) 2.185 (3), N(1)−B(1) 1.398 (6), N(1)−C(2) 1.416 (6), B(1)−C(3) 1.589 (6), B(1)−C(4) 1.587 (7), C(1)−Sn(1)−N(1) 115.2 (13), Sn(1)−N(1)−C(2) 124.7 (3), Sn(1)−N(1)−B(1) 114.8 (3), C(2)−N(1)−B(1) 119.6 (3), N(1)−B(1)−C(3) 123.0 (4), N(1)−B(1)−C(4) 121.1 (4), C(3)−B(1)−C(4) 115.9 (3).

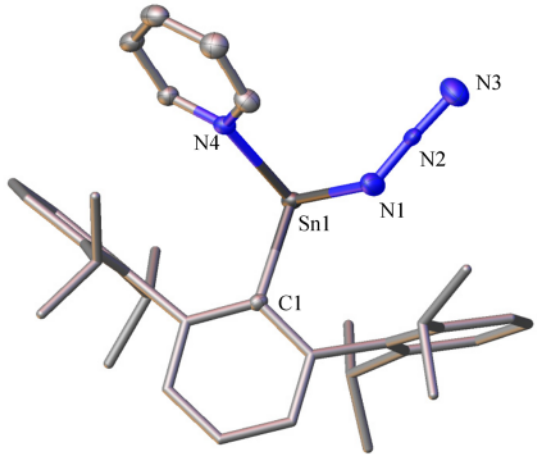

6

Figure 4. Drawing of the structure of $Ar^{iPr4}Sn(py)N_3$ (6). Thermal ellipsoids (50%) are shown for the core atoms. Hydrogen atoms are not shown. Selected bond lengths [Å] and bond angles [deg]: 6, C(1)−Sn(1) 2.227 (9), Sn(1)−N(1) 2.177 (11), Sn(1)−N(4) 2.343 (9), N(1)−N(2) 1.184 (5), N(2)−N(3) 1.183 (5), C(1)−Sn(1)−N(1) 93.2 (19), C(1)−Sn(1)−N(4) 100.1 (3), N(1)−Sn(1)−N(4) 83.4 (3), Sn(1)−N(1)−N(2) 119.6 (2), N(1)−N(2)−N(3) 169.9 (12).

long Sn(1)−N(4) distance of 2.343(9) Å, which is similar to that in the previously reported $Ar^{iPr6}Sn(py)Cl$ (2.369(4) Å).[45] The essentially equal N(1)−N(2) and N(2)−N(3) distances of 1.184 (5) and 1.183 (5) Å indicate the azido group exists as a −N=N=N isomer, cf. a difference of 0.13 Å in the −N−N≡N isomers in 2 and 3.

NMR Spectroscopy. The $^{119}Sn\{^1H\}$ NMR spectrum of 2 in C_6D_6 at room temperature displays a sharp signal at 418.2 ppm, which is significantly downfield-shifted in comparison to that of the bridged aryl/amido tin(II) species $[ArSn(\mu\text{-}NH_2)]_2$ (Ar = Ar^{iPr4} or Ar^{Me6}) (280 and 313 ppm). This may be due to the greater electron-donating character of the azido group.[46] The $^{119}Sn\{^1H\}$ NMR chemical shift for 3 is located at 241.5 ppm. This upfield location in comparison to 2 or the above-mentioned amides may be caused by the delocalized electron density of the N atom in the rings, which leads to the deshielding of the tin nucleus. Evidence of the formation of the azepinyl group is provided by the ^1H NMR spectrum. In contrast to the two doublets that represent two sets of methyl groups from the isopropyl groups of the terphenyl groups in 2, the ^1H NMR spectrum of 3 displays eight doublets, representing different electron environments for the eight methyl groups on each inserted ligand between 0.61 and 1.63 ppm.

The $^{119}Sn\{^1H\}$ NMR spectrum of 4 shows a sharp signal at 850.2 ppm, which is upfield-shifted in comparison to that of the previously reported aryl/amido stannylene, $Ar^{iPr6}Sn\{N(SiMe_3)_2\}_2$ (Ar^{iPr6} = C_6H_3-2,6-(C_6H_2-2,4,6-*i*-Pr_3)), of 1196.8 ppm,[47] and the 907.1 ppm chemical shift of the monobridged imido Sn(II) species $Me_3SiN(SnAr^{iPr4})_2$, both of which feature a two-coordinate tin(II) atom bound to an aryl group and a nitrogen.[48] A chemical shift at −4.14 ppm in the $^{11}B\{^1H\}$ NMR spectrum indicates a tetrahedrally coordinated B atom that, in this case, is bound to three C_6F_5 moieties and a N atom. It is similar to the −1.5 ppm of $(C_6F_5)_3B(NH_2CMe_3)$ and to the −3.6 ppm of $(2\text{-Me})C_5H_4NB(C_6F_5)_3$.[49,50] The equivalence of the three $-C_6F_5$ moieties was supported by the ^{19}F NMR spectrum which displays three signals at −132.2, −155.7, and −162.3 ppm for an integration ratio of 2:1:2, representing the ortho, para, and meta F atoms, respectively, which confirms the coordination of the BCF moiety.[51] The $^{119}Sn\{^1H\}$ NMR signal of 5 is observed at 1016.2 ppm consistent with two-coordinate tin.[52−54] The shift is similar to but is slightly upfield-shifted in comparison to that of the aryl/amido stannlyene $Ar^{iPr4}Sn\{N(SiMe_3)_2\}$ at 1196.8 ppm.[47] This may be due to the presence of the electron-withdrawing groups $-C_6F_5$ and $-B(C_6F_5)_2$ causing reduced electron density

DOI: 10.1021/acs.inorgchem.7b02413
Inorg. Chem. 2017, 56, 14596−14604

Scheme 3. Proposed Mechanism for the Formation of $[C_6H_3\text{-}2\text{-}(C_6H_3\text{-}2,6\text{-}^iPr_2)\text{-}6\text{-}(C_6H_3N\text{-}3,7\text{-}^iPr_2)Sn]_2$ (3) and $Ar^{iPr4}SnN(C_6F_5)B(C_6F_5)_2$ (5) via a Sn Nitride Intermediate

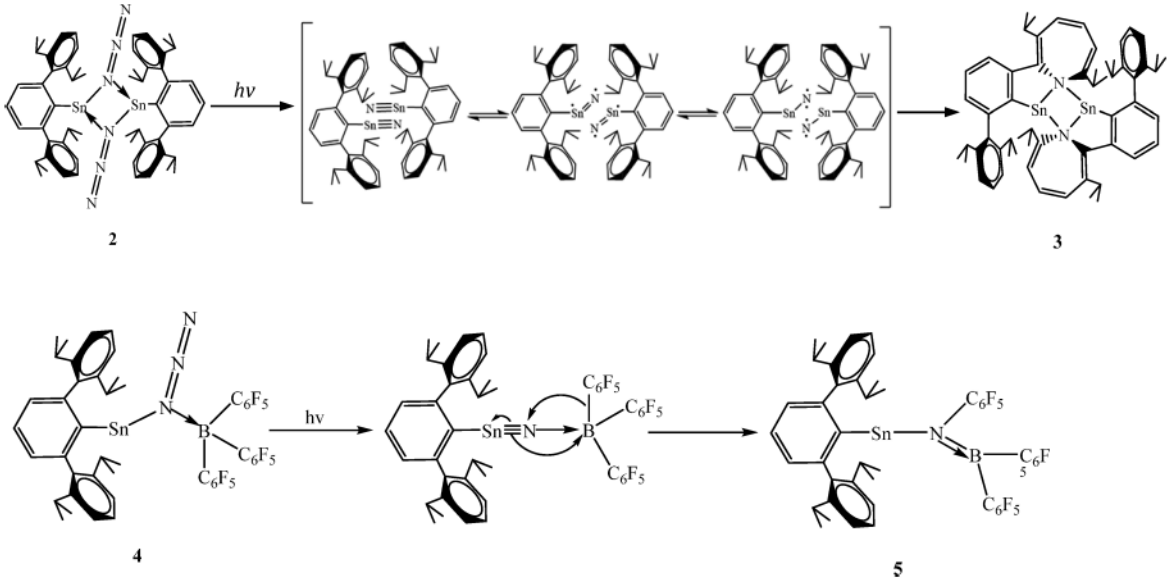

of the N atom. In the $^{11}B\{^1H\}$ NMR spectrum a singlet was observed to be downfield-shifted to 37.2 ppm in comparison to that in 4 as a consequence of the lower coordination number of the boron.[55] The ^{19}F NMR spectrum shows nine resonances between −131.6 and −162.3 ppm, representing different electron environments for the three $-C_6F_5$ rings confirming the rigidity of the nitrogen and boron coordination as well as the multiple character of the B−N bond.[55] A variable-temperature (VT) ^{19}F NMR study was performed with the object of observing free rotation of the B−N bond and cleavage of the donor−acceptor N═B π bond in 5. Increasing the temperature gradually to 90 °C shows no evidence of equilibration of the fluorine atom signals, indicating a strong N═B mutiple-bond character.

The ^1H NMR spectrum of 6 displays two triplet signals at 6.25 and 6.61 ppm and a doublet at 7.70 ppm with the integration ratio of 2:1:2, indicating the meta, para, and ortho H atoms of the coordinated pyridine. The $^{119}Sn\{^1H\}$ NMR spectrum shows a sharp signal at 256.7 ppm, which is downfield-shifted in comparison to that of $Ar^{iPr4}Sn(py)Cl$ (233.6 ppm) (see Supporting Information), which is due to the electron donation of the azido group.

Possible Tin Nitride Intermediates. The nature of the products 3 and 5 is suggestive of the existence of highly reactive intermediates generated by the photolysis. C−H bond activation by metal carbon or metal nitrogen multiple-bonded moieties have been reported. The "stannylcarbyne" $Ar^{iPr6}Sn{\equiv}C{-}Si^iPr_3$, which was generated as an intermediate by photolysis of the diazomethylstannylene $Ar^{iPr6}Sn{-}C(N_2)Si^iPr_3$, reacts as a carbene to insert into the C−H bond of the isopropyl group of the terphenyl ligand.[56] Furthermore, a uranium nitride intermediate "$(Cp^*)_2[N(SiMe_3)_2]U{\equiv}N$" was reported to insert into the C−H bond from the methyl group of the Cp* ligand.[57] A photoactivated nickel azido species, $Ni(N_3)PNP$ (PNP = 2,2′-di(isopropylphosphino)-4,4′-ditolylamide) was reported to react with the C−H bond of a benzene molecule via a transient nickel nitride intermediate, "PNPNi≡N".[58] However, instead of C−H activation of the ligand, the photolysis product of 2 displays C−C bond insertion involving a flanking C_6H_3-2,6-Pr^i_2 group. The addition of pyridine to 2 to form the complex 6 shuts down the photolysis activation shown by 2. This is presumably due to the blocking of the reaction pathway by the occupation of the tin p-orbital by the pyridine donor.

A parallel experimental investigation was performed by the addition of a strong Lewis acid, tris(pentafluorophenyl)borane (BCF), to complex the α-nitrogen of the azide and cause dissociation of the dimer with formation of 4.[42] The BCF-coordinated monomeric stannylene 4 was photolyzed for ca. 12 h. Unlike the photolysis of 6, this afforded the N_2 elimination and the insertion of the α-nitrogen atom into one of the B−C bonds to form 5, a derivative of a borylamido ligand (Figure 3). A rare example of such an insertion was reported by Mayer and co-workers with an osmium nitride species in which the Lewis acid BCF was added to the osmium nitride, $TpOs(N)Cl_2$ (Tp = hydrotris(3,5-dimethylpyrazol-1-yl)borato). The coordinated species then underwent a rearrangement in which one of the $-C_6F_5$ moieties migrates to the N atom to form the osmium amido compound $TpOs\{N(C_6F_5)B(C_6F_5)_2\}Cl_2$,[59] which further supports the existence of the reactive −Sn≡N triple -bonded intermediate.

In the proposed mechanism for the formation of 3 (Scheme 3, top), the monomeric Sn nitride is formed as a consequence of the N_2 elimination and then dimerizes to form the bridged species (shown within the large brackets). The reactive nitride may then react as an isomeric nitrene and attack a C−C bond of one of the flanking rings of the terphenyl ligand of the partner tin moiety to reform a dimeric species. The mechanism of the formation of 5 (Scheme 3, bottom) suggests that the nitride that is partly stabilized by the BCF acceptor molecule is formed. The electrons on the Sn−N π-bond of the intermediate are transferred to the electrophilic boron atom, which along with the σ-donation by the N atom, forms a B−N multiple bond. The $-C_6F_5$ group then migrates to the N atom to form an amido group with the reduction of the tin by the donation of the other pair of electrons in the Sn−N π-bond.

EPR Spectroscopy. Solutions of compound 2 or 4 were subjected to ca. 30 min of UV photolysis and then frozen to trap any potential intermediates. Analysis by EPR spectroscopy revealed that photolysis of 2 or 4 resulted in the formation of the same radical intermediate. The low-temperature (15 K) X-band EPR spectrum is shown in Figure 5 and Figure S1.

DOI: 10.1021/acs.inorgchem.7b02413
Inorg. Chem. 2017, 56, 14596−14604

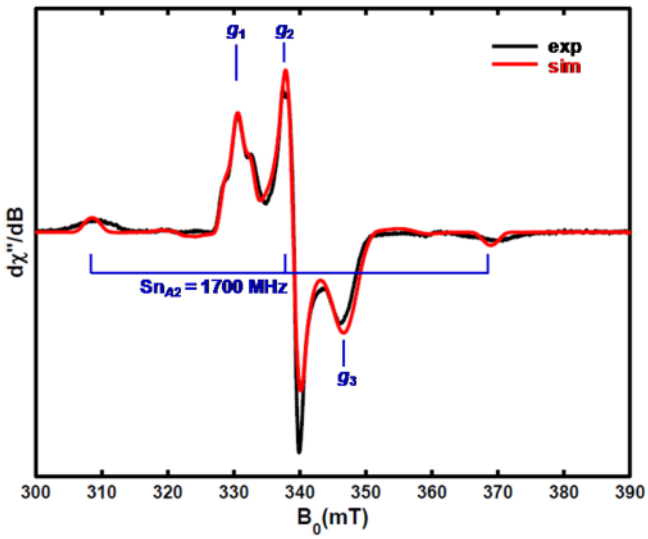

Figure 5. X-band CW EPR spectrum (black trace) of the radical intermediate trapped by UV photolysis of compound 2 in toluene for ~30 min. The spectrometer settings are as follows: 15 K, 0.1 mW power (no saturation), microwave frequency, 9.38 GHz, conversion time, 40 ms, modulation amplitude, 0.8 mT, modulation frequency, 100 kHz. The simulation (red trace) parameters are as follows: g = [2.029, 1.978, 1.933], A^{119}_{Sn} = [430, 1700, 650] MHz, A^{14}_{N} = [15, 15, 25] MHz and two equivalent ^{1}H nuclei with A^{1}_{H} = [50, 15, 45] MHz.

The temperature dependence of the EPR spectra (see Figure S2) suggests that this radical species is monomeric, as the intensity of signal behaves according to the Curie law except at very low temperature near 7 K, where the signal intensity is slightly low, which could be due to partial signal saturation. A significantly large hyperfine splitting of ~1700 MHz (60.7 mT) centered at the magnetic field of 339.1 mT (corresponding to g value 1.978) suggests that this radical species is a Sn-centered radical (^{119}Sn: I = 1/2, 8.59% abundance; ^{117}Sn: I = 1/2, 7.68% abundance), due to the strong Fermi contact and spin-dipolar interactions of electron spin with $^{117/119}$Sn nuclear spin.[60,61] This radical exhibits a rhombic g tensor with [g_1, g_2, g_3] = [2.029, 1.978, 1.933], and with g_{iso} = 1.992, which is in the range of the typical Sn-centered radicals.[62−65] The hyperfine tensor of ^{119}Sn was determined as [A_1, A_2, A_3] = [430, 1700, 650] MHz from simulation (see Figure S3 for more details), with A_{iso} = 926 MHz corresponding to 33.1 mT. Spin density analysis shows that there is ~0.55 spin population residing on tin in this trapped intermediate.[61] We did not observe two distinct sets of hyperfine splittings that are expected from the couplings of an unpaired electron with two isotope nuclei ^{119}Sn and ^{117}Sn with the gyromagnetic ratios of $\gamma(^{119}Sn)/\gamma(^{117}Sn) \approx 1.046$. This could be because the difference between $A(^{119}Sn)$ and $A(^{117}Sn)$ is small, resulting in the broad hyperfine peaks, as shown in Figure 5, with the overlap of hyperfine features from two different isotope nuclei.[66]

In addition, we observed significant superhyperfine splittings (ca. 1.8 mT) at the magnetic field of 330.6 mT (corresponding to g_1 2.029) with an intensity ratio of 1:2:1. These features could only be well-simulated by employing two equivalent ^{1}H nuclei (I = 1/2) with anisotropic hyperfine (A^{1}_{H}) tensors of [50, 15, 45] MHz, as well as one ^{14}N nucleus (I = 1) with an anisotropic hyperfine (A^{14}_{N}) tensor of [15, 15, 25] MHz (see Figure S4 for more details). This simulation is further confirmed by Q-band electron spin−echo detected field swept absorption spectrum and the corresponding pseudomodulated spectrum (Figure S5). This radical signal showed maximum intensity during the UV photolysis reaction (see Figure S6A), which first increased and then diminished as the reaction proceeded for longer than ca. 4 h, suggesting a reaction intermediate identity. We did not observe this radical intermediate upon UV photolysis of compound 6. It is likely that this intermediate is related to the nitride [−Sn^{IV}≡N] species in isomeric equilibrium with nitrene [−Sn^{II}−N] and nitridyl [−Sn^{III}═N·],[57,67] which can be generated by decomposition of tin azide with dinitrogen elimination under UV photolysis, followed by hydrogen atom transfer to quench much of the spin density on the nitrogen to form a possible doublet radical (S = 1/2) intermediates −Sn·═N(H).[68] Such an H atom abstraction explains why the ^{14}N hyperfine is rather small and is also observed for uranium nitride species.[57] The transferred hydrogen atoms are most likely from the methine protons of the -C_6H_3-2,6-$^{i}Pr_2$ ring, as we already ruled out the source from the solvent by using d_8-toluene, which show the same EPR spectrum (see Figure S7). Further investigations on this radical intermediate are underway.

■ CONCLUSION

The photolysis of a low-valent Sn(II) azide resulted in the insertion of a highly reactive nitrogen center into a carbon−carbon bond to yield [C_6H_3-2-(C_6H_3-2,6-$^{i}Pr_2$)-6-(C_6H_3N-3,7-$^{i}Pr_2$)Sn]$_2$ (3) or a carbon−boron bond in 4 to afford 5. EPR studies of the reactions suggested radical valence isomers of Ar^{iPr4}Sn≡N as reactive intermediates.

■ EXPERIMENTAL SECTION

General Procedures. All operations were performed under anaerobic and anhydrous conditions using modified Schlenk techniques. All solvents were dried over alumina columns and degassed prior to use. The ^{1}H, ^{13}C, and ^{119}Sn NMR spectroscopic data were collected on a Varian 600 MHz spectrometer. The ^{119}Sn NMR data were referenced to $SnBu_4$ (−11.7 ppm). Infrared spectra were collected as a mineral oil mull using a Bruker Tensor 27 IR spectrometer. [Ar^{iPr4}Sn(μ-Cl)]$_2$ (1) was synthesized according to literature methods.[69] NaN_3 and BCF were obtained from commercial sources, stored in the drybox, and used without further purification. Pyridine was dried over CaH_2 and trap-to-trap distilled prior to use.

Approximately 60 mM of compound 2 or 4 dissolved in either diethyl ether or toluene was prepared in a nitrogen-filled anhydrous glovebox and transferred to a quartz X-band (ID = 2.8 mm, OD = 3.8 mm) EPR tube that had a Teflon stopcock to keep the sample anaerobic. Then the sample was exposed under UV light at room temperature for ca. 30 min before being flash-frozen in liquid nitrogen.

The X-band (9.38 GHz) continuous-wave (CW) EPR spectra were recorded on a Bruker (Billerica, MA) EleXsys E500 spectrometer that was equipped with a superhigh Q resonator (ER4122SHQE). Cryogenic temperatures were achieved and controlled using an ESR900 liquid helium cryostat in conjunction with a temperature controller (Oxford Instruments ITC503) and gas flow controller. CW EPR data were collected under slow-passage, nonsaturating conditions. The spectrometer settings were as follows: conversion time = 40 ms, modulation amplitude = 0.3 mT, and modulation frequency = 100 kHz; other settings are given in corresponding figure captions.

A Q-Band two-pulse electron spin−echo (ESE)-detected field-swept EPR spectrum ($\pi/2$-τ−π−τ-echo) was collected at 34.220 GHz using a Bruker (Billerica, MA) EleXsys E580 spectrometer equipped with a 1 W amplifier and a R.A. Isaacson cylindrical TE011 resonator in an Oxford CF935 cryostat. Pulse sequences were programmed with the PulseSPEL programmer via the XEPR interface. Experiment parameters: 10 K, microwave frequency = 34.220 GHz, $\pi/2$ = 12 ns, and τ = 300 ns. Spectral simulations were performed using the Easyspin 5.1.10 toolbox[70,71] within the MatLab software suite (The Mathworks Inc., Natick, MA).

[Ar^{iPr4}Sn(μ-N_3)]$_2$ (2). A mixture of [Ar^{iPr4}Sn(μ-Cl)]$_2$ (0.46 g, 0.834 mmol) and NaN_3 (0.081 g, 1.25 mmol) was added to ca. 30 mL of diethyl ether.

DOI: 10.1021/acs.inorgchem.7b02413
Inorg. Chem. 2017, 56, 14596−14604

The solution color changed from dark orange to pale orange over 1 h of rapid stirring at ca. 25 °C. The solution was allowed to stir for a further 16 h, and the solvent was removed under reduced pressure. The product was extracted with toluene (ca. 5 mL) and then stored at ca. −18 °C to afford **2** as colorless crystals. Yield: 0.39 g (85%), mp 148−150 °C; ^{1}H NMR (600 MHz, C_6D_6, 298 K): δ = 1.02 (d, 24H, ^3J = 6.9 Hz, $CH(CH_3)_2$), 1.32 (d, 24H, ^3J = 6.9 Hz, $CH(CH_3)_2$), 3.01 (sept, 6H, ^3J = 6.9 Hz, $CH(CH_3)_2$), 7.03−7.14 (m, 12H, *m*-C_6H_3, *p*-C_6H_3, *m*-Dipp and *p*-Dipp; Dipp = 2,6-^{i}Pr$_2$−C_6H_3) ppm; ^{13}C{^{1}H} NMR (C_6D_6, 125 MHz, 298 K): δ = 23.3, 26.3, 30.9, 123.6, 129.2, 130.6, 139.2, 146.7, 147.3 ppm; ^{119}Sn{^{1}H} NMR (C_6D_6,223.6 MHz, 298 K): δ = 418.2 ppm; IR (CsI, mineral oil; selected, cm^{-1}): 2080 (N_3 stretching), 450, 380.

[C$_6$H$_3$-2-(C$_6$H$_3$-2,6-^{i}Pr$_2$)-6-(C$_6$H$_3$N-3,7-^{i}Pr$_2$)Sn]$_2$ ***(3)***. Compound **2** (0.35 g, 0.625 mmol) was dissolved in diethyl ether (ca. 20 mL) at room temperature. The solution was transferred to a quartz tube and exposed under UV light for 16 h. The pale orange solution became dark orange in color. The solution was concentrated to ca. 5 mL under reduced pressure and then stored at ca. −18 °C to afford **3** as colorless crystals. Yield: 0.28 g (84%), mp 144−146 °C; ^{1}H NMR (600 MHz, C_6D_6, 298 K): δ = 0.61 (d, 6H, ^3J = 6.9 Hz, $CH(CH_3)_2$), 0.76 (d, 6H, ^3J = 6.9 Hz, $CH(CH_3)_2$), 0.89 (d, 6H, ^3J = 6.9 Hz, $CH(CH_3)_2$), 1.06 (d, 6H, ^3J = 6.9 Hz, $CH(CH_3)_2$), 1.16 (d, 6H, ^3J = 6.9 Hz, $CH(CH_3)_2$), 1.36 (d, 6H, ^3J = 6.9 Hz, $CH(CH_3)_2$), 1.40 (d, 6H, ^3J = 6.9 Hz, $CH(CH_3)_2$), 1.63 (d, 6H, ^3J = 6.9 Hz, $CH(CH_3)_2$), 2.38 (sept, 2H, ^3J = 6.9 Hz, $CH(CH_3)_2$), 3.09 (sept, 6H, ^3J = 6.9 Hz, $CH(CH_3)_2$), 3.41 (sept, 6H, ^3J = 6.9 Hz, $CH(CH_3)_2$), 3.43 (sept, 6H, ^3J = 6.9 Hz, $CH(CH_3)_2$), 5.84−7.45 (m, 18H, *m*-C_6H_3, *p*-C_6H_3, *m*-Dipp and *p*-Dipp; Dipp = 2,6-^{i}Pr$_2$−C_6H_3) ppm; ^{13}C{^{1}H} NMR (C_6D_6, 125 MHz, 298 K): δ = 21.1. 22.0, 23.1, 23.2, 24.7, 26.5, 28.6, 29.8, 30.7, 31.5, 37.7, 117.2, 123.1, 123.4, 126.3, 127.0, 128.5, 129.9, 135.4, 138.5, 141.6, 144.4, 145.6, 146.6, 157.3, 178.3 ppm; ^{119}Sn{^{1}H} NMR (C_6D_6,223.6 MHz, 298 K): δ = 241.5 ppm; IR (CsI, mineral oil; Selected, cm^{-1}): 450, 380.

Ar^{iPr4}SnN$_3$B(C$_6$F$_5$)$_3$ ***(4)***. To a rapidly stirred solution of **2** (0.43 g, 0.780 mmol) in diethyl ether (ca. 30 mL) was added B(C_6F_5)$_3$ (0.40 g, 0.780 mmol) in diethyl ether (ca. 15 mL). The solution color changed from pale orange to yellow. After it had been continuously stirred for 12 h, the solution was concentrated under reduced pressure to ca. 5 mL. Storing the concentrated solution at ca. −18 °C afforded **4** as colorless crystals. Yield: 0.74 g (89%); mp 158−160 °C; ^{1}H NMR (600 MHz, C_6D_6, 298 K): δ = 0.87 (d, 12H, ^3J = 6.9 Hz, $CH(CH_3)_2$), 1.17 (d, 12H, ^3J = 6.9 Hz, $CH(CH_3)_2$), 2.86 (sept, 4H, ^3J = 6.9 Hz, $CH(CH_3)_2$), 6.98−7.38 (m, 9H, *m*-C_6H_3, *p*-C_6H_3, *m*-Dipp and *p*-Dipp; Dipp = 2,6-^{i}Pr$_2$−C_6H_3) ppm; ^{13}C{^{1}H} NMR (C_6D_6, 125 MHz, 298 K): δ = 22.3, 31.3, 122.9, 125.1, 125.7, 128.6, 131.0, 146.9 ppm; ^{11}B{^{1}H} NMR (C_6D_6, 128.3 MHz, 298 K): δ = −4.6 ppm; ^{19}F NMR (C_6D_6, 376.3 MHz, 298 K): δ = −132.2 (b, 6F, *ortho*-C_6F_5), −155.6 (b, 3F, *para*-C_6F_5), −162.3 (b, 6F, *meta*-C_6F_5) ppm; ^{119}Sn{^{1}H} NMR (C_6D_6,223.6 MHz, 298 K): δ = 850.2 ppm; IR (CsI, mineral oil; selected, cm^{-1}): 2100 (N_3 stretching) 450, 360.

Ar^{iPr4}SnN(C$_6$F$_5$)B(C$_6$F$_5$)$_2$ ***(5)***. A solution of **4** (0.3 g, 0.585 mmol) in diethyl ether (ca. 20 mL) was transferred to a quartz tube and exposed under UV light for ca. 12 h. The solution changed color from pale orange to dark orange. It was concentrated to ca. 5 mL under reduced pressure and then stored at ca. −18 °C to afford **5** as colorless crystals. Yield: 0.26 g (92%); mp 155−158 °C; ^{1}H NMR (600 MHz, C_6D_6, 298 K): δ = 0.87 (d, 12H, ^3J = 6.9 Hz, $CH(CH_3)_2$), 1.12 (d, 12H, ^3J = 6.9 Hz, $CH(CH_3)_2$), 2.82 (sept, 4H, ^3J = 6.9 Hz, $CH(CH_3)_2$), 6.92−7.37 (m, 9H, *m*-C_6H_3, *p*-C_6H_3, *m*-Dipp and *p*-Dipp; Dipp = 2,6-^{i}Pr$_2$−C_6H_3) ppm; ^{13}C{^{1}H} NMR (C_6D_6, 125 MHz, 298 K): δ = 23.9, 30.3, 122.4, 128.0, 131.0, 139.2, 140.7, 146.4; ^{11}B{^{1}H} NMR (C_6D_6, 128.3 MHz, 298 K): δ = 37.2 ppm; ^{19}F NMR (C_6D_6, 376.3 MHz, 298 K): δ = −131.9 (d, 2F, *ortho*-C_6F_5), −133.1 (d, 2F, *meta*-C_6F_5), −147.9 (t, 1F, *para*-C_6F_5), −148.4 (d, 2F, *ortho*-C_6F_5), −148.9 (t, 1F, *para*-C_6F_5), −156.2 (t, 1F, *para*-C_6F_5), −160.5 (m, 2F, *para*-C_6F_5), −160.9 (m, 2F, *ortho*-C_6F_5), −161.9 (d, 2F, *ortho*-C_6F_5) ppm; ^{119}Sn{^{1}H} NMR (C_6D_6,223.6 MHz, 298 K): δ = 1016.2 ppm; IR (CsI, mineral oil; selected, cm^{-1}): 2100 (N_3 stretching) 450, 380.

Ar^{iPr4}Sn(py)N$_3$ ***(6)***. To a rapidly stirred solution of **2** (0.54 g, 0.965 mmol) in toluene (ca. 30 mL) was added pyridine (0.07 mL, 1.06 mmol) via syringe. The solution color changed from light orange to pale yellow immediately after the addition. After the solution was allowed to stir for 1 h, it was concentrated under reduced pressure to ca. 3 mL under dynamic vacuum. Colorless crystals of **6** were obtained after storing the solution at ca. −18 °C for 12 h. mp 145−150 °C; ^{1}H NMR (600 MHz, C_6D_6, 298 K): δ = 1.07 (d, 12H, ^3J = 6.9 Hz, $CH(CH_3)_2$), 1.28 (d, 12H, ^3J = 6.9 Hz, $CH(CH_3)_2$), 3.14 (sept, 4H, ^3J = 6.9 Hz, $CH(CH_3)_2$), 6.26 (t, 2H, ^3J = 6.6 Hz, *meta*-py-H), 6.61 (t, 1H, ^3J = 6.6 Hz, *para*-py-H), 6.99−7.24 (m, 9H, *m*-C_6H_3, *p*-C_6H_3, *m*-Dipp and *p*-Dipp; Dipp = 2,6-^{i}Pr$_2$−C_6H_3), 7.70 (d, 2H, ^3J = 6.6 Hz, *ortho*-py-H) ppm; ^{13}C{^{1}H} NMR (C_6D_6, 125 MHz, 298 K): δ = 23.0, 26.1, 31.1, 123.1, 124.6, 126.8, 128.3, 128.9, 137.9, 147.5, 148.2 ppm; ^{119}Sn{^{1}H} NMR (C_6D_6,223.6 MHz, 298 K): δ = 256.7 ppm; IR (CsI, mineral oil; selected, cm^{-1}): 2050 (N_3 stretching) 450, 350.

■ ASSOCIATED CONTENT

Supporting Information

The Supporting Information is available free of charge on the ACS Publications website at DOI: 10.1021/acs.inorgchem.7b02413.

Selected X-ray crystallographic data for **2**−**6**, X-band CW EPR spectra, temperature dependence of EPR spectra, simulations of X-band CW EPR spectra, Q-band electron spin-echo detected field swept absorption spectrum, various NMR spectra, FT-IR data for **2**−**6** (PDF)

Accession Codes

CCDC 1574402−1574407 contain the supplementary crystallographic data for this paper. These data can be obtained free of charge via www.ccdc.cam.ac.uk/data_request/cif, or by emailing data_request@ccdc.cam.ac.uk, or by contacting The Cambridge Crystallographic Data Centre, 12 Union Road, Cambridge CB2 1EZ, UK; fax: +44 1223 336033.

■ AUTHOR INFORMATION

Corresponding Author

*Fax: +1-530-732-8995. Phone: +1-530-752-6913. E-mail: pppower@ucdavis.edu.

ORCID

Troy A. Stich: 0000-0003-0710-1456
Marilyn M. Olmstead: 0000-0002-6160-1622
R. David Britt: 0000-0003-0889-8436
Philip P. Power: 0000-0002-6262-3209

Notes

The authors declare no competing financial interest.

■ ACKNOWLEDGMENTS

We wish to acknowledge the U.S. Department of Energy (DE-FG02-07ER4675) office of Basic Energy Sciences for support of this work. We thank the National Science Foundation (Grant Nos. CHE-0840444, 1263760, 1531193, 1565501, and 1665455) for support of two dual-source X-ray diffractometers and the EPR spectrometer.

■ REFERENCES

(1) Audrieth, L. F. Hydrazoic Acid and Its Inorganic Derivatives. *Chem. Rev.* 1934, *15*, 169−224.

(2) Adhikary, C.; Koner, S. Structural and Magnetic Studies on Copper(II) Azido Complexes. *Coord. Chem. Rev.* 2010, *254*, 2933−2958.

(3) Ribas, J.; Escuer, A.; Monfort, M.; Vicente, R.; Cortés, R.; Lezama, L.; Rojo, T. Polynuclear NiII and MnII Azido Bridging Complexes. Structural Trends and Magnetic Behavior. *Coord. Chem. Rev.* 1999, *193*, 1027−1068.

(4) Evans, B. L.; Yoffe, A. D.; Gray, P. Physics And Chemistry Of The Inorganic Azides. *Chem. Rev.* 1959, *59*, 515−568.

DOI: 10.1021/acs.inorgchem.7b02413
Inorg. Chem. 2017, 56, 14596−14604

(5) Strähle, J. Reactions of Transition Metal Azido Complexes and their Reaction Products. *Z. Anorg. Allg. Chem.* **2007**, *633*, 1757−1761.
(6) Dehnicke, K.; Strähle, J. Über Molybdännitridchlorid $Cl_3Mo{\equiv}N$ und Wolframnitridchlorid $Cl_3W{\equiv}N$. *Z. Anorg. Allg. Chem.* **1965**, *339*, 171−181.
(7) Bezler, H.; Strähle, J. Preparation and Crystal Strucutre of Niobium(Triphenyl-Phosphineimino)Teracholoride, $Nb[NP(C_6H_5)_3]Cl_4$, a Compound with a Niobium Nitrogen Multiple Bond. *Z. Naturforsch. B* **1979**, *34*, 1199−1202.
(8) Bezler, H.; Strähle, J. Über die Staudinger-Reaktion mit Tantaltetrachloridazid. Die Kristallstruktur von Tantal (V)-(triphenyl-phosphinimino) tetrachlorid, $Ta[NP(C_6H_5)_3]Cl_4$/On the Staudinger Reaction with Tantalum Tetrachloride Azide. The Crystal Structure of Tantalum (V)(triphenyl-phosphinimino) tetrachloride, $Ta[NP(C_6H_5)_3]Cl_4$. *Z. Naturforsch., B: J. Chem. Sci.* **1983**, *38*, 317−320.
(9) Strähle, J. Synthesis of Cluster Compounds by Photolysis of Azido Complexes. *J. Organomet. Chem.* **1995**, *488*, 15−24.
(10) Shekar, S.; Twamley, B.; Wehmschulte, R. J. Facile Synthesis of Monoazidotitanium Isopropoxides. *Inorg. Chem.* **2008**, *47*, 10804−10806.
(11) Curtius, T. Ueber Stickstoffwasserstoffsäure (Azoimid) N_3H. *Ber. Dtsch. Chem. Ges.* **1890**, *23*, 3023−3033.
(12) Reichle, W. T. Preparation, Properties, and Thermal Decomposition Products of Organoazides of Silicon, Germanium, Tin, Lead, Phosphorus, and Sulfur. *Inorg. Chem.* **1964**, *3*, 402−406.
(13) Parker, D. R.; Sommer, L. H. Pyrolysis of Silyl Azides. Generation and Reactions of Unsaturated Silicon-Nitrogen Intermediates $[R_2Si = NR]$. *J. Organomet. Chem.* **1976**, *110*, C1−C4.
(14) Chassaing, S.; Sani Souna Sido, A.; Alix, A.; Kumarraja, M.; Pale, P.; Sommer, J. Click Chemistry" in Zeolites: Copper(I) Zeolites as New Heterogeneous and Ligand-Free Catalysts for the Huisgen [3 + 2] Cycloaddition. *Chem. - Eur. J.* **2008**, *14*, 6713−6721.
(15) Raj, P.; Ranjan, A.; Singhal, K. Cycloaddition Reactions of Unsaturated Substrates with a Germanium Nitrogen Bond. *Synth. React. Inorg. Met.-Org. Chem.* **1984**, *14*, 477−484.
(16) Svec, P.; Bartos, K.; Ruzickova, Z.; Curinova, P.; Dusek, L.; Turek, J.; De Proft, F.; Ruzicka, A. C,N-Chelated Organotin(IV) Azides: Synthesis, Structure and Use within Click Chemistry. *New J. Chem.* **2016**, *40*, 5808−5817.
(17) Filippou, A. C.; Portius, P.; Kociok-Kohn, G. Germanium(II) Azides: Synthesis and Crystal Structure of $Tp'GeN_3$ [Tp' = hydrotris-(3,5-dimethylpyrazol-1-yl)borato]. *Chem. Commun.* **1998**, 2327−2328.
(18) Ayers, A. E.; Marynick, D. S.; Dias, H. V. R. Azido Derivatives of Low-Valent Group 14 Elements: Synthesis, Characterization, and Electronic Structure of $[(n\text{-}Pr)_2ATI]GeN_3$ and $[(n\text{-}Pr)_2ATI]SnN_3$ Featuring Heterobicyclic 10-π-Electron Ring Systems. *Inorg. Chem.* **2000**, *39*, 4147−4151.
(19) Ayers, A. E.; Klapötke, T. M.; Dias, H. V. R. Azido Derivatives of Germanium(II) and Tin(II): Syntheses and Characterization of $[(Mes)_2DAP]GeN_3$, $[(Mes)_2DAP]SnN_3$, and the Corresponding Chloro Analogues Featuring Heterocyclic Six-π-Electron Ring Systems (where $[(Mes)_2DAP] = \{N(Mes)C(Me)\}_2CH$). *Inorg. Chem.* **2001**, *40*, 1000−1005.
(20) Veith, M.; Rammo, A. Darstellung und Reaktivitätsuntersuchungen an Einem Intramolekular Basenstabilisierten Germanium(II)-Azid. *Z. Anorg. Allg. Chem.* **2001**, *627*, 662−668.
(21) Dias, H. V. R.; Ayers, A. E. Reactions of Divalent Group 14 Compounds Containing an Azide Functionality: Synthesis and Characterization of $[HB(3,5\text{-}(CF_3)_2Pz)_3]AgGe(N_3)[(n\text{-}Pr)_2ATI]$ and $[HB(3,5\text{-}(CF_3)_2Pz)_3]AgSn(N_3)[(n\text{-}Pr)_2ATI]$. *Polyhedron* **2002**, *21*, 611−618.
(22) Ochiai, T.; Franz, D.; Irran, E.; Inoue, S. Formation of an Imino-Stabilized Cyclic Tin(II) Cation from an Amino(imino)stannylene. *Chem. - Eur. J.* **2015**, *21*, 6704−6707.
(23) Dehnicke, K.; Strähle, J. The Transition Metal-Nitrogen Multiple Bond. *Angew. Chem., Int. Ed. Engl.* **1981**, *20*, 413−426.
(24) Dehnicke, K.; Liese, W.; Kohler, P. Rhenium(VI) Nitridochloride, $ReNCl_3$. *Z. Naturforsch., B: J. Chem. Sci.* **1977**, *32*, 1487.
(25) Fritzsche, J.; Struve, H. Ueber die Osman-Osmiumsäure. *J. Prakt. Chem.* **1847**, *41*, 97−113.
(26) Frank, K.-P.; Strahle, J.; Weidlein, J. Preparation, Vibrational Spectra and Crystal Structure of the Deca Bromo μ-Nitrido Ditantalate-(V) $Ta_2NBr_{10}^{3-}$. A Complex with a Symmetrical Ta = N=Ta Bridge. *Z. Naturforsch., B: J. Chem. Sci.* **1980**, *35*, 300.
(27) Liese, W.; Dehnicke, K. New Syntheses of $ReNCl_3$. *Z. Naturforsch., B: J. Chem. Sci.* **1978**, *33*, 1061.
(28) Dehnicke, K.; Liese, W.; Kohler, P. Rhenium(VI) Nitridochloride, $ReNCl_3$. *Z. Naturforsch., B: J. Chem. Sci.* **1977**, *32*, 1484.
(29) Chatt, J.; Rowe, G. A. 788. Complex Compounds of Tertiary Phosphines and a Tertiary Arsine with Rhenium(V), Rhenium(III), and Rhenium(II). *J. Chem. Soc.* **1962**, 4019−4033.
(30) Chatt, J.; Garforth, J. D.; Johnson, N. P.; Rowe, G. A. 196. Nitrido- and Arylimido-Complexes of Rhenium. *J. Chem. Soc.* **1964**, 1012−1020.
(31) King, D. M.; Tuna, F.; McInnes, E. J. L.; McMaster, J.; Lewis, W.; Blake, A. J.; Liddle, S. T. Isolation and Characterization of a Uranium(VI)−Nitride Triple Bond. *Nat. Chem.* **2013**, *5*, 482−488.
(32) Niecke, E.; Nieger, M.; Reichert, F. Arylmino(halogeno)-phosphanes XP = $NC_6H_2tBu_3$ (X = Cl, Br, I) and the Iminophosphenium Tetrachloroaluminate $[P{\equiv}NC_6H_2tBu_3]{\oplus}[AlCl_4]{\ominus}$: the First Stable Compound with a PN Triple Bond. *Angew. Chem., Int. Ed. Engl.* **1988**, *27*, 1715−1716.
(33) Yoshimura, T.; Hamada, K.; Imado, M.; Hamata, K.; Tomoda, K.; Fujii, T.; Morita, H.; Shimasaki, C.; Ono, S.; Tsukurimichi, E.; Furukawa, N.; Kimura, T. First Preparation and X-ray Crystallographic Structure Determination of S,S,S-Triphenylthiazyne. *J. Org. Chem.* **1997**, *62*, 3802−3803.
(34) Baldas, J.; Colmanet, S.; Williams, G. Preparation and Structure of Dibromobis(N,N-diethyldithiocarbamato)-thionitrosyltechnetium-(III). *Aust. J. Chem.* **1991**, *44*, 1125−1132.
(35) Wu, A.; Dehestani, A.; Saganic, E.; Crevier, T. J.; Kaminsky, W.; Cohen, D. E.; Mayer, J. M. Reactions of Tp−Os Nitrido Complexes with the Nucleophiles Hydroxide and Thiosulfate. *Inorg. Chim. Acta* **2006**, *359*, 2842−2849.
(36) Behrens, U.; Petersen, J.; Lork, E.; Watson, P. G.; Mews, R. $[L_3Ni(\mu\text{-}L)_3NiL_3](AsF_6)_4$, (L = $N{\equiv}SF_2NMe_2$), a Dinuclear Nickel Complex with Bridging Thiazyl(dimethylamide)difluoride Ligands. *Angew. Chem., Int. Ed. Engl.* **1997**, *36*, 1878−1879.
(37) Gau, D.; Nougué, R.; Saffon-Merceron, N.; Baceiredo, A.; De Cózar, A.; Cossío, F. P.; Hashizume, D.; Kato, T. Donor-Stabilized 1,3-Disila-2,4-diazacyclobutadiene with a Nonbonded Si···Si Distance Compressed to a Si = Si Double Bond Length. *Angew. Chem., Int. Ed.* **2016**, *55*, 14673−14677.
(38) Jutzi, P.; Neumann, B.; Reumann, G.; Stammler, H.-G. Novel Ga_2N_2 Ring Systems by Reaction of Pentamethylcyclopentadienylgallium with Organic Azides. *Organometallics* **1999**, *18*, 2037−2039.
(39) Eyster, E. H. The Spectrum of Allene in the Photographic Infra-Red. *J. Chem. Phys.* **1938**, *6*, 580−585.
(40) Owens, R. G.; Barker, E. F. The Infra-Red Absorption Spectrum of Methyl Amine. *J. Chem. Phys.* **1940**, *8*, 229−232.
(41) Herbert, D. E.; Lara, N. C.; Agapie, T. Arene C-H Amination at Nickel in Terphenyl−Diphosphine Complexes with Labile Metal−Arene Interactions. *Chem. - Eur. J.* **2013**, *19*, 16453−16460.
(42) Camp, C.; Grant, L. N.; Bergman, R. G.; Arnold, J. Photo-Activation of d^0 Niobium Imido Azides: en Route to Nitrido Complexes. *Chem. Commun.* **2016**, *52*, 5538−5541.
(43) Herbert, D. E.; Lara, N. C.; Agapie, T. Arene C = H Amination at Nickel in Terphenyl−Diphosphine Complexes with Labile Metal−Arene Interactions. *Chem. - Eur. J.* **2013**, *19*, 16453−16460.
(44) Wang, X.; Ni, C.; Zhu, Z.; Fettinger, J. C.; Power, P. P. N−H and N = C Bond Formation via Germanium(III) Diradicaloid Intermediates and C−S Bond Cleavage in Reactions of the Digermyne Ar′GeGeAr′ (Ar′ = C_6H_3-2,6-$(C_6H_3$-2,6-$Pr^{i2})_2$) with Azides. *Inorg. Chem.* **2009**, *48*, 2464−2470.
(45) Eichler, B. E.; Pu, L.; Stender, M.; Power, P. P. The Synthesis and Structure of Sterically Encumbered Terphenyl Tin(II) Halide Derivatives: Simultaneous Existence of Monomers and Dimers in the Crystalline Phase. *Polyhedron* **2001**, *20*, 551−556.

DOI: 10.1021/acs.inorgchem.7b02413
Inorg. Chem. 2017, 56, 14596−14604

(46) Peng, Y.; Brynda, M.; Ellis, B. D.; Fettinger, J. C.; Rivard, E.; Power, P. P. Addition of H_2 to Distannynes under Ambient Conditions. *Chem. Commun.* **2008**, 6042−6044.
(47) Pu, L.; Olmstead, M. M.; Power, P. P.; Schiemenz, B. Synthesis and Characterization of the Monomeric Terphenyl−Metal Halides Ge(Cl){C_6H_3-2,6-$Trip_2$} (Trip = C_6H_2-2,4,6-*i*-Pr_3) and Sn(I){C_6H_3-2,6-$Trip_2$} and the Terphenyl−Metal Amide Sn{$N(SiMe_3)_2$}{C_6H_3-2,6-$Trip_2$}. *Organometallics* **1998**, *17*, 5602−5606.
(48) Cui, C.; Olmstead, M. M.; Fettinger, J. C.; Spikes, G. H.; Power, P. P. Reactions of the Heavier Group 14 Element Alkyne Analogues Ar'EEAr' (Ar' = C_6H_3-2,6(C_6H_3-2,6-Pr^{i}_2)$_2$; E = Ge, Sn) with Unsaturated Molecules: Probing the Character of the EE Multiple Bonds. *J. Am. Chem. Soc.* **2005**, *127*, 17530−17541.
(49) Lancaster, S. J.; Mountford, A. J.; Hughes, D. L.; Schormann, M.; Bochmann, M. Ansa-Metallocenes with B-N and B-P Linkages: the Importance of N-H···F-C Hydrogen Bonding in Pentafluorophenyl Boron Compounds. *J. Organomet. Chem.* **2003**, *680*, 193−205.
(50) Geier, S. J.; Gille, A. L.; Gilbert, T. M.; Stephan, D. W. From Classical Adducts to Frustrated Lewis Pairs: Steric Effects in the Interactions of Pyridines and $B(C_6F_5)_3$. *Inorg. Chem.* **2009**, *48*, 10466−10474.
(51) Massey, A. G.; Park, A. J. Perfluorophenyl Derivatives of the Elements. *J. Organomet. Chem.* **1966**, *5*, 218−225.
(52) Spikes, G. H.; Peng, Y.; Fettinger, J. C.; Power, P. P. Synthesis and Characterization of the Monomeric Sterically Encumbered Diaryls E{C_6H_3-2,6-(C_6H_3-2,6-Pr^{i}_2)$_2$}$_2$ (E = Ge, Sn, or Pb). *Z. Anorg. Allg. Chem.* **2006**, *632*, 1005−1010.
(53) Phillips, A. D.; Hino, S.; Power, P. P. A Reversible Valence Equilibrium in a Heavier Main Group Compound. *J. Am. Chem. Soc.* **2003**, *125*, 7520−7521.
(54) Lei, H.; Fettinger, J. C.; Power, P. P. Synthesis and Structures of Low-Valent Alkynyl Tin and Germanium Complexes Supported by Terphenyl Ligands: Heavier Group 14 Element Enediyne Analogues. *Organometallics* **2010**, *29*, 5585−5590.
(55) Reiß, F.; Schulz, A.; Villinger, A. Synthesis, Structure, and Reactivity of Diazene Adducts: Isolation of iso-Diazene Stabilized as a Borane Adduct. *Chem. - Eur. J.* **2014**, *20*, 11800−11811.
(56) Setaka, W.; Hirai, K.; Tomioka, H.; Sakamoto, K.; Kira, M. Stannaacetylene (RSn⋮CR') Showing Carbene-like Reaction Mode. *J. Am. Chem. Soc.* **2004**, *126*, 2696−2697.
(57) Thomson, R. K.; Cantat, T.; Scott, B. L.; Morris, D. E.; Batista, E. R.; Kiplinger, J. L. Uranium azide photolysis results in C−H bond activation and provides evidence for a terminal uranium nitride. *Nat. Chem.* **2010**, *2*, 723−729.
(58) Vreeken, V.; Siegler, M. A.; de Bruin, B.; Reek, J. N. H.; Lutz, M.; van der Vlugt, J. I. C-H Activation of Benzene by a Photoactivated NiII(azide): Formation of a Transient Nickel Nitrido Complex. *Angew. Chem.* **2015**, *127*, 7161−7165.
(59) Crevier, T. J.; Bennett, B. K.; Soper, J. D.; Bowman, J. A.; Dehestani, A.; Hrovat, D. A.; Lovell, S.; Kaminsky, W.; Mayer, J. M. C−N Bond Formation on Addition of Aryl Carbanions to the Electrophilic Nitrido Ligand in $TpOs(N)Cl_2$. *J. Am. Chem. Soc.* **2001**, *123*, 1059−1071.
(60) Morton, J.; Preston, K. Atomic parameters for paramagnetic resonance data. *J. Magn. Reson.* **1978**, *30*, 577−582.
(61) "The Fermi-contact and spin-dipolar interactions of electron spin with ^{119}Sn nuclear spin refer to the isotropic hyperfine interaction of unit spin in 5s orbital (^{119}Sn: a_{iso} = −43 910 MHz) and the anisotropic hyperfine interaction of unit spin in 5p orbital (^{119}Sn: P = −1831 MHz).[60] The hyperfine tensor of ^{119}Sn in the radical intermediate is determined as [A_1, A_2, A_3] = [430, 1700, 650] MHz, with A_{iso} = 926 MHz and T = 387 MHz. The spin density (ρ) on ^{119}Sn is calculated by using $A_{iso} = \rho_{5s}a_{iso}$; $T = -2/5\rho_{5p}P$, giving ρ_{5s} = 0.02 and ρ_{5P} = 0.53.".
(62) Becker, M.; Förster, C.; Franzen, C.; Hartrath, J.; Kirsten, E.; Knuth, J.; Klinkhammer, K. W.; Sharma, A.; Hinderberger, D. Persistent Radicals of Trivalent Tin and Lead. *Inorg. Chem.* **2008**, *47*, 9965−9978.
(63) Iley, J. The Chemistry of Organic Germanium. In *Tin and Lead Compounds;* Patai, S., Ed.; John Wiley & Sons Ltd.: New York, 1995.
(64) Kurzbach, D.; Yao, S.; Hinderberger, D.; Klinkhammer, K. W. EPR Spectroscopic Characterization of Persistent Germyl-substituted Pb(III)- and Sn(III)-radicals. *Dalton. Trans.* **2010**, *39*, 6449−6459.
(65) Jackel, G. S.; Gordy, W. Electron Spin Resonance of Free Radicals Formed from Group-IV and Group-V Hydrides in Inert Matrices at Low Temperature. *Phys. Rev.* **1968**, *176*, 443.
(66) EasySpin automatically simulates the spectra of all possible isotopologues (isotopes combinations) and combines them with the appropriate weights. For Sn-based hyperfine interactions, it will first compute a "^{119}Sn" spectrum using the reported hyperfine values. Then by scaling the ^{119}Sn hyperfine values by the gyromagnetic ratios of $\gamma(^{119}Sn)/\gamma(^{117}Sn)$ and using this hyperfine interaction in the simulation, the "^{117}Sn" spectrum is obtained. The resultant simulated spectrum is achieved by summing these two data sets together once they are scaled by the percent natural abundance of each isotope.
(67) Scheibel, M. G.; Askevold, B.; Heinemann, F. W.; Reijerse, E. J.; de Bruin, B.; Schneider, S. Closed-shell and Open-shell Square-planar Iridium Nitrido Complexes. *Nat. Chem.* **2012**, *4*, 552−558.
(68) The hyperfine tensor of ^{14}N is [15, 15, 25] MHz, with A_{iso} = 18.3 MHz and T = 3.3 MHz. The spin density (ρ) on ^{14}N is calculated by using a_{iso} = 1811 MHz and P = 138.8 MHz and the equations: $A_{iso} = \rho_{2s}a_{iso}$; $T = -2/5\rho_{2p}P$, giving ρ_{2s} = 0.01 and ρ_{2p} = 0.06. Similarly, the spin density on each of the ^{1}H is calculated to be ρ_{1s} = 0.025. Therefore, ∼0.33 spin density is delocalized to the phenyl ring.
(69) Pu, L.; Phillips, A. D.; Richards, A. F.; Stender, M.; Simons, R. S.; Olmstead, M. M.; Power, P. P. Germanium and Tin Analogues of Alkynes and Their Reduction Products. *J. Am. Chem. Soc.* **2003**, *125*, 11626−11636.
(70) Stoll, S.; Britt, R. D. General and Efficient Simulation of Pulse EPR Spectra. *Phys. Chem. Chem. Phys.* **2009**, *11*, 6614−6625.
(71) Stoll, S.; Schweiger, A. EasySpin, a Comprehensive Software Package for Spectral Simulation and Analysis in EPR. *J. Magn. Reson.* **2006**, *178*, 42−55.

DOI: 10.1021/acs.inorgchem.7b02413
Inorg. Chem. 2017, 56, 14596−14604